A Comprehensive Study of an Acid-Based Reversible H_2-Br_2 Fuel Cell System

Venkata Yarlagadda,[a,*] Regis P. Dowd, Jr.,[a,*] Jun Woo Park,[b,*] Peter N. Pintauro,[b,] and Trung Van Nguyen[a,**,z]**

[a]*Department of Chemical and Petroleum Engineering, The University of Kansas, Lawrence, Kansas 66045, USA*
[b]*Department of Chemical and Biomolecular Engineering, Vanderbilt University, Nashville, Tennessee 37212, USA*

The regenerative H_2-Br_2 fuel cell has been a subject of notable interest and is considered as one of the suitable candidates for large scale electrical energy storage. In this study, the preliminary performance of a H_2-Br_2 fuel cell using both conventional as well as novel materials (Nafion and electrospun composite membranes along with Pt and Rh_xS_y electrocatalysts) is discussed. The performance of the H_2-Br_2 fuel cell obtained with a conventional Nafion membrane and Pt electrocatalyst was enhanced upon employing a double-layer Br_2 electrode while raising the cell temperature to 45°C. The active area and wetting characteristics of Br_2 electrodes were improved upon by either pre-treating with HBr or boiling them in de-ionized water. On the other hand, similar or better performances were obtained using dual fiber electrospun composite membranes (PFSA/PPSU) versus using Nafion membranes. The Rh_xS_y electrocatalyst proved to be more stable in the presence of HBr/Br_2 than pure Pt. However, the H_2 oxidation activity on Rh_xS_y is quite low compared to that of Pt. In conclusion, a stable H_2 electrocatalyst that can match the hydrogen oxidation activity obtained with Pt and a membrane with low Br_2/Br^- permeability are essential to prolong the lifetime of a H_2-Br_2 fuel cell.
 [DOI: 10.1149/2.1041508jes] All rights reserved.

Manuscript submitted February 20, 2015; revised manuscript received May 12, 2015. Published June 6, 2015. This was Paper 1339 presented at the San Francisco, California, Meeting of the Society, October 27–November 1, 2013.

Electrochemical energy storage using flow batteries or reversible fuel cell devices are considered feasible options for taking advantage of renewable energy sources such as wind and solar.[1–4] An ideal reversible fuel cell should possess qualities such as swift reaction kinetics, inexpensive reactants, high round trip efficiency, and durability. Several research efforts conducted in this area have identified the reversible hydrogen-bromine (H_2-Br_2) fuel cell as a suitable system for large scale electrical energy storage because of its numerous advantages such as rapid Br_2 and H_2 reaction kinetics, low cost ($1-$3 per kg of hydrobromic acid), and relative abundance of the active materials used in this system.[5–13] However, the toxicity and corrosivity of the HBr/Br_2 electrolyte used in this system pose major safety and durability challenges that need to be addressed.

A conventional H_2-Br_2 fuel cell consists of a H_2 electrode and a Br_2 electrode separated by a proton exchange membrane. However, microporous membrane and membrane-less versions of several fuel cell systems have been investigated.[13–15] Recently, Braff et al. developed a membrane-less version of the H_2-Br_2 flow battery to reduce the cost and ease the hydration requirements associated with the system.[13] The starting material in the H_2-Br_2 fuel cell system is hydrobromic acid (HBr). With excess energy from either wind or solar, the HBr solution is electrolyzed to form H_2 and Br_2 at their respective electrodes (charge process) and the process is reversed during discharge. Also, the bromide (Br^-) ion in the solution may react with neutral bromine (Br_2) species to form a tri-bromide (Br_3^-) complex. The electrochemical reactions involved in this fuel cell system are shown below.

$$H_2 \text{ electrode: } H_2 \underset{\text{charge}}{\overset{\text{discharge}}{\rightleftarrows}} 2H^+ + 2e^- \qquad E^o = 0\,V$$

$$Br_2 \text{ electrode: } Br_2 + 2e^- \underset{\text{charge}}{\overset{\text{discharge}}{\rightleftarrows}} 2Br^- \qquad E^o = 1.09\,V$$

$$\text{Overall: } \quad H_2 + Br_2 \underset{\text{charge}}{\overset{\text{discharge}}{\rightleftarrows}} 2HBr \qquad E^o = 1.09\,V$$

The H_2-Br_2 fuel cell has been extensively studied in the past highlighting numerous advantages and some limitations of the system.[5–13]

Despite the numerous attractive features offered by the H_2-Br_2 fuel cell, there are some major material-related challenges that need to be solved to bring this system to commercialization. During fuel cell operation, especially in the charge direction, there is a possibility of species such as bromine (Br_2), bromide (Br^-), and tri-bromide (Br_3^-) crossing over to the H_2 electrode through the polymer electrolyte membrane due to electroosmotic drag. Subsequently, this will poison and corrode the platinum (Pt) catalyst. The crossover may severely affect the fuel cell performance. Fuel cell lifetime is reduced as the rate of crossover increases. There are two possible approaches to limit the effect of crossover. The first approach is to use a membrane that is impermeable to bromine, bromide, and tri-bromide cross over. The second approach is to use an alternative H_2 catalyst with similar activity as Pt that is stable in the HBr/Br_2 environment. Several previous studies have explored using electrospun nanofiber composite membranes (usually a blend of inert polymer and Nafion) for proton exchange membrane (PEM) and direct methanol fuel cells in order to address issues such as the excessive swelling and high permeability of commercially available Nafion membranes.[16–18]

An optimum membrane should have high conductivity and ionic selectivity as well as be resistant to negative hydration effects. The negative hydration effects can be explained as follows. When the PEM is not hydrated, the transport of protons across the membrane effectively goes to zero due to the incomplete dissociation of ionic groups ($-SO_3^-H^+$) within the membrane.[19] When a membrane is overly hydrated, the polymer swells causing the ionic pathways through the membrane to open up and allow larger chemical species to diffuse across the membrane. The ionic selectivity has been shown to change drastically with the relative hydration of the PEM.[20] The purpose of making electrospun composite membranes is to create a sufficient number of ionic pathways available for protons to move through the membrane, while also physically preventing the membrane from swelling at high relative humidity. Even though the electrospun composite membranes reduce the crossover of unwanted species, it is challenging to fabricate a membrane that can completely prevent the crossover of unwanted species while also allowing for sufficient ionic conductivity of desired species. However, the electrospun composite membrane may reduce the rate of crossover enough to prolong the life of catalyst materials used in the fuel cell. In conclusion, an active H_2 electrocatalyst stable in HBr/Br_2 environment is still needed to avoid any negative impact of crossover species on the H_2-Br_2 fuel cell performance.

*Electrochemical Society Student Member.
**Electrochemical Society Fellow.
zE-mail: CPTVN@KU.EDU

Prior works have shown that the instability of Pt catalyst material in HBr/Br_2 environment was due to blockage of active sites (poisoning) and dissolution of catalyst material (corrosion).[21,22] The poisoning effect is reversible and thus can be mitigated to a certain extent by holding the H_2 electrode at hydrogen evolution potentials. However, the corrosion effect is irreversible and hence the catalyst material that decomposes over time cannot be recovered. Several previous works have screened transition metal chalcogenides as oxygen reduction catalysts for hydrochloric acid (HCl) electrolysis and conventional direct methanol fuel cells (DMFC).[23,24] Of the transition metal chalcogenides investigated, rhodium sulfide (Rh_xS_y) was identified as one of the stable and active electrocatalysts for the oxygen reduction reaction in the presence of a corrosive acidic environment.[23–27] Similarly, the activity of H_2 reactions on transition metal sulfides was examined in some of the previous works as well.[28,29] The Rh_xS_y catalyst was also found to be a stable (in HBr/Br_2 environment) and active electrocatalyst for hydrogen evolution reaction during HBr electrolysis.[22,29,30] Even though some of the other transition metal sulfides such as cobalt ruthenium sulfide ($Co_{1-x}Ru_xS_2$), ruthenium sulfide (RuS_2), and tungsten disulfide (WS_2) were stable in highly corrosive HBr/Br_2 solutions, their hydrogen evolution reaction and hydrogen oxidation reaction (HER/HOR) activity was too low to be considered as active electrocatalysts.[29]

The Rh_xS_y electrocatalyst is composed of multiple phases such as Rh_2S_3, Rh, Rh_3S_4, and $Rh_{17}S_{15}$. Prior works have identified metallic Rh, $Rh_{17}S_{15}$ and Rh_3S_4 to be the likely active phases for HER/HOR.[23,25] Since the price of Rh is equally high as platinum, the only advantage it offers is its stability. An alternate approach to reduce the impact of crossover is to alter the fuel cell system design or operation to allow platinum to be used as a feasible electrocatalyst. For example, Cho et al. claims that maintaining the hydrogen electrode at a hydrogen evolution potential or a continuous flow of H_2 gas through the hydrogen electrode prevents Pt catalyst poisoning by bromine and bromide ions.[31] However, even the leverage provided by smart system design or operation may still fail in situations such as emergency system shut down or loss of hydrogen environment. The best possible solution to avoid the impact of crossover is to develop a stable electrocatalyst with decent activity for hydrogen reactions.

In this communication, preliminary fuel cell test results with conventional Nafion membranes and Pt electrocatalysts are discussed in the first section. The preliminary results include the effect of Br_2 electrode pretreatment, fuel cell operating temperature, and Br_2 electrode thickness on the H_2-Br_2 fuel cell performance. The second section focuses on studies involving the performance evaluation of electrospun composite membranes and the stability of Pt and Rh_xS_y (BASF) electrocatalysts in an actual fuel cell fixture.

Experimental

An elaborate description of the H_2-Br_2 fuel cell assembly was described in our previous work.[32] A plain SGL carbon (10AA) gas diffusion layer (GDL) was used as the Br_2 electrode and a bi-layer carbon gas diffusion medium (SGL 35BC) coated with Pt/C or Rh_xS_y (BASF)/C was used as the hydrogen electrode. The Pt electrode was obtained from TVN systems, Inc., and the Rh_xS_y electrode was prepared by painting a solution of Rh_xS_y/C and Nafion on the microporous layer (MPL) of the bi-layer carbon gas diffusion medium with a brush. The catalyst (Pt or Rh_xS_y) loading in the hydrogen electrode was approximately 0.5 mg/cm^2. The membrane electrode assemblies (MEAs) were made with commercially available Nafion (212 and 115) and electrospun composite membranes. A 2M HBr/2M Br_2 electrolyte mixture was fed to the Br_2 electrode in the H_2-Br_2 fuel cell experiments that examine the effect of pretreated Br_2 electrodes, fuel cell operating temperature, Br_2 electrode thickness, and electrospun composite membranes. A 2M HBr/1M Br_2 electrolyte mixture was fed to the Br_2 electrode for the catalyst stability studies. H_2 gas at 122 kPa was recirculated through the H_2 electrode. The H_2 and HBr/Br_2 pump flow rates were 1380 cm^3/min (or 97.2 A/cm^2 equivalent current density) and 1.5 cm^3/min (or 4.3 A/cm^2 equivalent current density for 2M Br_2 and 2.15 A/cm^2 equivalent current density for 1M Br_2 during discharge) respectively. Interdigitated flow fields were used for all the experimental studies. Also, liquid water at a flow rate of 0.05 cm^3/min was injected into the H_2 side to humidify the H_2 gas which facilitated hydration of the ionomer phase in the hydrogen electrode.[33] All the experiments were conducted at room temperature (~22°C) unless otherwise specified. At the end of each experiment, the internal ohmic resistance of the fuel cell was acquired using Electrochemical Impedance Spectroscopy (Gamry EIS 300, Amplitude: 5 mV and Frequency range: 0.1 Hz to 100 kHz).

The preliminary H_2-Br_2 fuel cell studies involve three different sections. First, the effect of pretreated Br_2 electrodes (SGL 10AA carbon electrodes soaked in 2M HBr and boiled in DI water) on the H_2-Br_2 fuel cell performance was examined. Second, the effect of temperature (25°C and 45°C) on the fuel cell performance was investigated. Finally, the effect of Br_2 electrode thickness (390 μm and 780 μm) was studied. For all the preliminary studies, a bi-layer porous carbon electrode (SGL 35BC) with Pt catalyst was used as the H_2 electrode.

The dual fiber electrospun composite membranes used in this study are composed of 55 vol. % Nafion perfluorosulfonic (PFSA) acid ionomer and 45 vol. % inert (uncharged) polyphenylsulfone (PPSU) polymer. The electrospun membrane characterized in this study was made by allowing the inert polymer (PPSU) to soften, flow, and fill the void space between PFSA nanofibers.[34,35] The inert polymer (PPSU) was used to control the swelling of the ionic Nafion phase, which in turn helped in reducing the crossover of unwanted species across the membrane. The fabrication process and transport properties of these composite membranes (PFSA/PPSU) were described elsewhere.[34] To identify differences in morphology, phase contrast, and conductivity between electrospun and commercial Nafion membranes, atomic force microscopy (AFM) was used. The ability to characterize the surface of the electrospun membranes is important to identify the PFSA ionic fibers that promote proton transport and the inert PPSU fibers that prevent the PEM from swelling. It is hypothesized that there will be a high correlation between the phase contrast and spreading resistance (conductivity) modes. Also, we expect that the ionic phase of the membrane surface to be more viscoelastic and adhesive than the inert phase.

A Veeco AFM Bioscope with Nanoscope Controller and a Nanosurf FlexAFM were used in contact and tapping modes in order to measure the morphology, phase contrast, and conductivity for electrospun (PFSA/PPSU) and Nafion 212 membranes. Both AFMs were used to verify measurement readings and reproducibility. Prior to and after each AFM measurement, highly-oriented pyrolytic graphite (HOPG) and a calibration grid were used to ensure proper AFM calibration and to verify tip durability throughout the experiment. In order to accurately measure the conductivity (or resistivity) of the membrane, a platinum coated cantilever was used to apply a voltage bias to the surface of the membrane. One side of the membranes was hot pressed onto a platinum coated SGL35BC gas diffusion electrode made by TVN Systems, Inc. The MEAs were made by hot pressing a membrane onto the gas diffusion layer (GDL) at 551.6 kPa and 285°F for 5 minutes. The AFMs were operated inside electrically shielded Faraday cages and on vibration isolation tables to minimize background noise while conducting the measurements. The experimental setup used for spreading resistance mode was described in previous studies conducted by our group.[36,37] Finally, the performance of dual fiber electrospun composite membranes was evaluated in an actual fuel cell fixture at 25°C and 45°C.

The stability of Pt and Rh_xS_y electrocatalysts was determined through accelerated testing. Initially, two fuel cell stacks with Pt and Rh_xS_y as H_2 electrode catalysts were assembled and the stability study was conducted over a week's period of time. On day 1, the fuel cell polarization (discharge and charge) curves were obtained for both stacks and, subsequently, the H_2 flow was secured (no flow) to the hydrogen electrode with HBr/Br_2 electrolyte stored in the Br_2 electrode. The hydrogen side was not pressurized (ambient conditions) thus allowing the HBr/Br_2 electrolyte to slowly diffuse through the membrane to

the H_2 electrode and interact with the catalyst layer. The fuel cell performance was acquired on odd numbered days (1, 3, 5, and 7) with the polarization curves obtained on day 1 being the initial performance. Between the consecutive runs, the stacks were stored with HBr/Br_2 electrolyte present in the Br_2 electrode and H_2 electrode at ambient conditions. This test is considered to be a highly severe accelerated test because the catalyst on the hydrogen side was neither protected by hydrogen or by cathodic protection. Note that while bromine is much more corrosive to a metal than bromide, in the presence of hydrogen it is quickly converted to bromide. Furthermore, it has been reported that bromide adsorption is voltage dependent. At voltages more negative than +60 mV of the hydrogen standard equilibrium potential, hydrogen is more preferentially adsorbed than bromide.[39] So, platinum can be protected by maintaining high hydrogen adsorption level, by using pressurized hydrogen on platinum at open circuit voltage condition or by applying a sufficiently negative overpotential to the platinum electrode (i.e., cathodic protection).

The next study was aimed at examining the feasibility of Pt as a H_2 electrocatalyst under the following fuel cell testing conditions. In the first case, the initial performance of the H_2-Br_2 fuel cell was measured and the system was allowed to sit at rest condition for 8 hours with the H_2 flow terminated (similar to the testing condition described above). After 8 hours, the performance of the fuel cell was measured again to check whether there is any impact of crossover on the performance. The second case study was performed under similar conditions as described above, but with a minor change. During this experiment, the H_2 pump was allowed to run with the H_2 gas recirculating at 122 kPa for the next 8 hours after measuring the initial performance. The HBr/Br_2 pump was stopped during the rest condition for both fuel cell stacks. The final test looked at the effect of HBr/Br_2 crossover in real time, while the fuel cell is operating in the discharge regime. In this experiment, the fuel cell was operated at a constant discharge potential (in this case at 0.8 V). After reaching a steady state current at the chosen discharge potential, a small volume of 2M HBr solution was injected into the hydrogen electrode. As soon as a small drop of 2M HBr entered the electrode, the H_2 pump was secured with the H_2 side still pressurized at 122 kPa. The fuel cell was maintained at OCV for approximately 8 minutes to allow the HBr to interact with the H_2 electrode. After 8 minutes, the discharge current of the fuel cell was measured at 0.8 V for another 10 to 12 minutes to observe whether there was any impact on performance due to Br^- in the H_2 electrode. Next, a mixture of 2M HBr/1M Br_2 was injected into the hydrogen electrode and the same procedure explained above for the HBr injection was implemented to examine the effect of Br^- and Br_2 crossover on the fuel cell performance. The HBr/Br_2 pump was operated continuously during the entire experiment.

Results and Discussion

Effect of pretreated Br_2 electrodes on fuel cell performance.— The aim of the electrode pretreatment is to increase the hydrophilicity and active surface area of the Br_2 carbon electrodes. To examine the effect of pretreated Br_2 electrodes on fuel cell performance, three different experiments were conducted. Initially, fuel cell performance was obtained using 2 layers of dry SGL 10AA carbon electrodes. The SGL 10AA carbon electrodes were boiled in DI water and soaked in 2M HBr for subsequent experiments. Nafion 212 membranes were used in the MEAs developed for this study. The HBr/Br_2 electrolyte and humidified H_2 gas were recirculated through the Br_2 and H_2 electrodes respectively for 30 minutes to hydrate the dry MEA prior to measuring the fuel cell performance. The presence of aqueous HBr electrolyte next to the membrane helps to quickly hydrate the cell and obtain stable performance. Figure 1 compares the performance of a H_2-Br_2 fuel cell acquired with pretreated and untreated carbon electrodes. As shown in Figure 1, the fuel cell discharge performance obtained with untreated (dry) carbon electrodes in the second run is higher compared to that in the first run (maximum discharge power density of 0.58 W/cm^2 obtained in second run compared to 0.49 W/cm^2 obtained in first run). The discharge performance in the first run is low over the whole discharge regime. During the first run, the electrodes were dry and hence hydrophobic to a certain extent. As a result, the reactants may not be able to access the entire active area of the carbon electrodes. As the first run progressed, the active area and wetting property of the carbon electrodes increased with their continuous exposure to HBr/Br_2 electrolyte solution. The first run acts like an acid pretreatment step for the carbon electrodes. Also note that when an interdigitated flow field is used, the electrolyte is forced to flow through the porous electrode. This configuration forces the electrolyte to penetrate into the carbon material and assist in wetting the carbon surface. For flow-by electrodes using parallel-straight channels where the electrolyte is not forced to flow through the electrodes, it may take much longer time for the carbon surface to become wetted. Furthermore, we believe that the passage of current may lead to surface chemical modifications and increased wetting in two ways. First, the electrolyte may be forced into the bromine electrode region that was not previously wetted during charge and discharge. Second, the bromine/bromide reaction may alter the carbon material surface to make it more wetted. Hence, the discharge performance of the H_2-Br_2 fuel cell with dry SGL 10AA carbon electrodes shows improvement in the second run. The fuel cell discharge performance curves obtained with the carbon electrodes boiled in DI water and those soaked in 2M HBr in the first run are similar and match reasonably well with those of the untreated carbon electrodes obtained in the second run. A similar performance improvement was observed by Cho et al. when using porous carbon electrodes pretreated with sulfuric acid instead of untreated ones.[9]

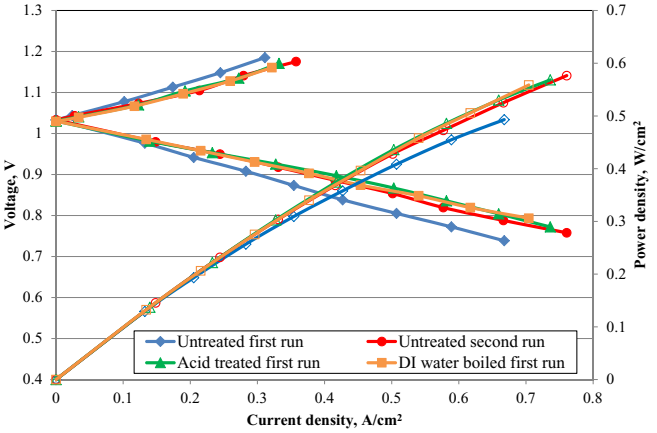

Figure 1. Effect of Br_2 electrode pretreatment (untreated, acid treated, and DI water boiled) on the H_2-Br_2 fuel cell performance (voltage: solid markers and power density: open markers) at room temperature (~22°C).

The major conclusion based on these experimental results is that the untreated carbon electrodes generate the same discharge performance as pretreated electrodes but after multiple discharge and charge cycles. The number of discharge and charge cycles required to condition the untreated carbon electrodes may go up as the electrode thickness increases. Thus, pre-treating the carbon electrodes prior to use assists with the HBr/Br_2 electrolyte gaining access to most of the active area immediately. Also, similar discharge performances obtained with carbon electrodes boiled in DI water and acid soaked in 2M HBr suggests that the wetting characteristic of an electrode plays a significant role in enhancing the area accessible to the aqueous reactants, and either treatment method can be used to achieve this effect. We recommend that regardless of the type of carbon electrode used, one should always try to pre-treat it in order to promote wetting and allow for high fuel cell performance to be achieved right away.

Effect of temperature on the fuel cell performance.— The performance of a H_2-Br_2 fuel cell can be enhanced in several ways. One such way is to boost the H_2 and Br_2 reaction kinetics as well as the transport processes inside the electrodes by increasing the fuel cell operating

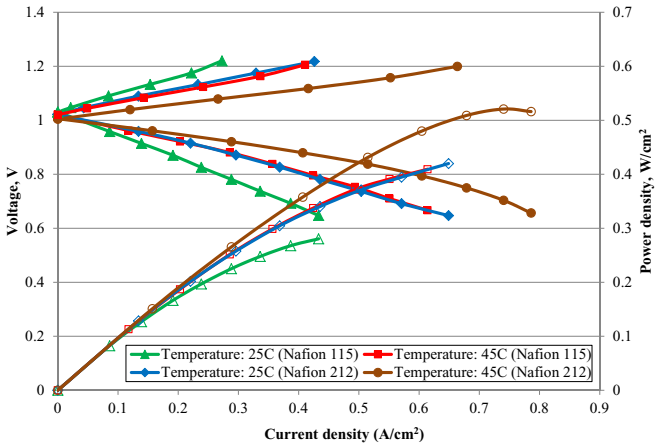

Figure 2. Effect of temperature (25°C and 45°C) and membrane (Nafion 212 and Nafion 115) thickness on H_2-Br_2 fuel cell performance (voltage: solid markers and power density: open markers).

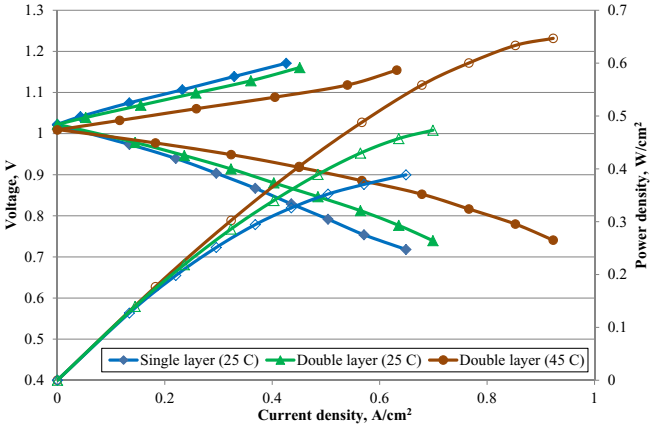

Figure 3. Effect of Br_2 electrode thickness (single layer: 390 μm at 25°C and double layer: 780 μm at 25°C and 45°C) on H_2-Br_2 fuel cell performance (voltage: solid markers and power density: open markers).

temperature. A similar study was conducted in our previous work but with uneven temperature control across the fuel cell fixture.[10] In this study, the H_2 gas entering the fuel cell, HBr/Br_2 electrolyte, and the fuel cell were heated to the same temperature in order to minimize the temperature gradient across the fuel cell stack. Figure 2 shows the results of the H_2-Br_2 fuel cell temperature studies with Nafion 212 and Nafion 115 membranes. The fuel cell performance is significantly improved in both the kinetic and mass transport controlled regions as the temperature increases from 25°C to 45°C. The internal ohmic resistance for the fuel cell with Nafion 212 membrane decreased by 28% as the temperature was raised from 25°C to 45°C (0.18 Ω-cm^2 at 25°C versus 0.13 Ω-cm^2 at 45°C). A similar decrease in internal ohmic resistance at higher temperatures was observed for the fuel cell with Nafion 115 membrane (0.4 Ω-cm^2 at 25°C versus 0.3 Ω-cm^2 at 45°C) as well. The decrease in ohmic resistance can be attributed to improvement in the diffusivity of reactant species and Nafion conductivity. In other words, molecular and ionic transport were significantly enhanced. The fuel cell performance at 45°C is increased compared to our prior study (Maximum power density of 0.52 W/cm^2 in this study versus 0.46 W/cm^2 in our previous study for the case where Nafion 212 membrane was used). Also, the fuel cell performance was enhanced by using a thinner membrane. Even though the performance of the fuel cell decreases with a thicker membrane, the crossover rate of Br_2 and Br^- species may be lowered. The performance trends shown in Figure 2 also match reasonably well with the previous studies.[8–11]

Effect of Br_2 electrode thickness on the fuel cell performance.— The H_2-Br_2 fuel cell performance can also be increased by increasing the Br_2 electrode thickness in this case because the commercial gas diffusion media used in fuel cells have very low specific surface areas. Figure 3 compares the performance of a fuel cell with two different electrode thicknesses, 390 μm (one piece of SGL 10AA electrode) and 780 μm (two pieces of SGL 10AA carbon electrode) respectively. The bromine electrode thickness in this study was increased by adding an additional SGL 10AA carbon electrode. The two SGL 10AA carbon electrodes were stacked together to increase the electrode thickness. The rest of the fuel cell configuration remains unchanged. The active area of the Br_2 electrode improves upon increasing the electrode thickness. In other words, the number of reaction sites increases, which is evident from the improvement in the fuel cell performance upon employing a thicker Br_2 electrode. An 18% increase in maximum power density was observed upon adding an additional Br_2 electrode at 25°C. The increase in the ohmic loss by adding an additional bromine electrode was insignificant relative to the power density gain (ohmic resistance increased by 6 mΩ upon adding an additional bromine electrode at 25°C). The interdigitated flow fields, which have shown to provide the best utilization of the electrode area, were used in these cells because of its flow-through versus flow-by characteristics of other flow fields such as the straight-parallel-channel and serpentine-channel flow fields.[10] As shown in Figure 3, the performance of the fuel cell can be further enhanced by operating the fuel cell with a thicker electrode at a higher temperature (two layers of SGL 10AA carbon electrodes at 45°C). A peak power density of 0.65 W/cm^2 was obtained with the thicker Br_2 electrode at 45°C.

Based on a previous modeling study conducted on the H_2-Br_2 fuel cell system, increasing the electrode layers beyond a certain limit may result in diffusion limited performance due to the increase in the ionic and molecular diffusion pathways.[32] An alternate approach that can increase the active surface area without affecting the transport related morphological properties like porosity and tortuosity of the electrode is to grow nanotubes directly onto the electrode fiber surface to create high active surface area.[38] This is a more suitable option compared to using a multi-layered carbon electrode approach because the electrode surface area can be improved without affecting the porosity/tortuosity or the electrode thickness.

Composite membrane studies.— In this study, the performance of dual fiber electrospun composite membranes consisting of 55 vol. % PFSA and 45 vol. % PPSU were evaluated in an actual fuel cell at 25°C and 45°C respectively. The thicknesses of the membrane samples evaluated were 25 μm (area specific resistance equivalent to that of Nafion 212 membrane) and 65 μm (area specific resistance equivalent to that of Nafion 115 membrane) respectively. Previous study conducted in this area have shown that the diffusivity and steady state permeability of bromine species in the composite membranes listed above was lower compared to that of commercially available Nafion membranes.[34] The 25 micron thick electrospun and Nafion 212 membranes were used in the AFM study. Figures 4 and 5 show the side-by-side comparison of three dimensional (3D) morphology, phase contrast, and conductivity of Nafion and dual fiber electrospun composite membranes. The electrospun membrane's morphology was consistently smoother than Nafion 212 as shown in Figure 4a. As expected, the phase contrast measurement of Nafion 212 was more uniform than the electrospun membranes. The PFSA nanofibers within the electrospun membranes can be easily recognized using either phase contrast or spreading resistance modes. The non-uniformity of the phase contrast and spreading resistance images for the electrospun membrane was due to the use of two different types of polymers, one ionic and the other inert. The ionic polymer used in the electrospun membrane is expected to exhibit a larger phase contrast than the inert polymer due to higher adhesive properties. As expected, the phase contrast measurement of Nafion 212 shows a surface with varying amounts of ionic clusters due to the migration of the ionic groups ($-SO_3^-H^+$)

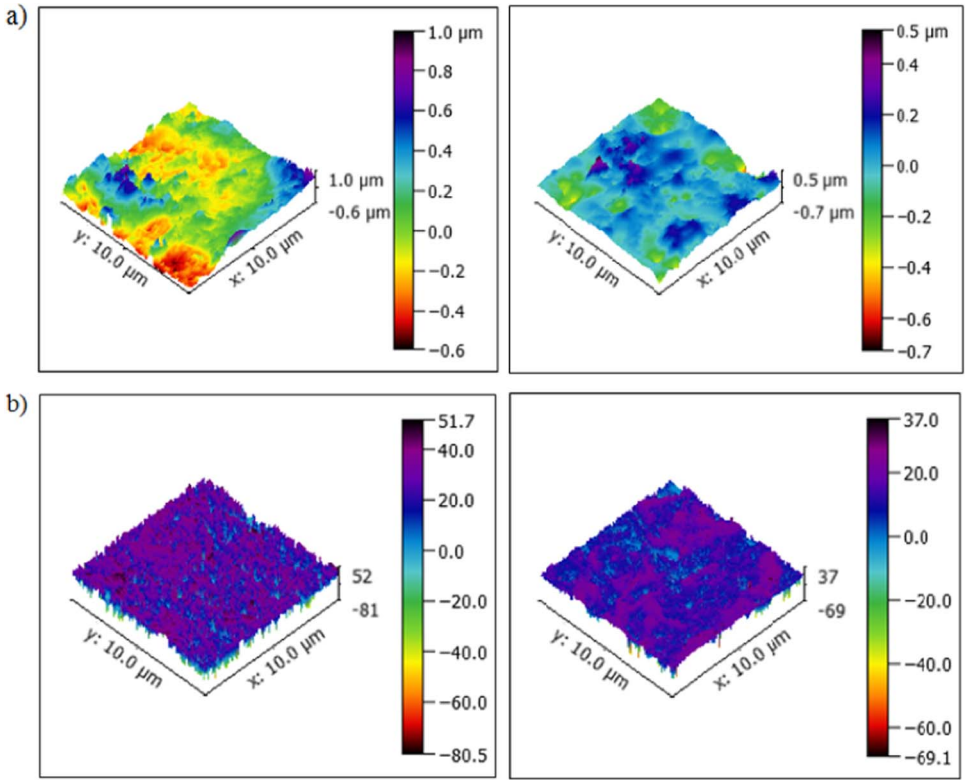

Figure 4. AFM images showing a) Morphology and b) Phase contrast of Nafion (left) and dual fiber electrospun composite membrane (right) with color scales representing the heights.

within the polymer to the membrane's surface. The movement of the ionic groups to the surface is probably due to plasticization combined with the tendency to reduce surface tension.

The purple (in color) or darker shaded region in Figure 4b (left image) correspond to areas with a larger number of ionic groups ($-SO_3^-H^+$); whereas the lighter domains correspond to areas rich in the fluorocarbon backbone structure of Nafion 212. The softer ionic groups are expected to have a larger phase contrast value due to the increased amount of surface/tip interactions (i.e. elasticity, viscoelasticity, adhesion, etc.). For the electrospun membrane, this was due to the difference in properties between the ionic fibers and the inert polymer matrix. The purple (in color) or darker shaded region in Figure 4b (right image) corresponds to the ionic fibers; whereas the lighter domains correspond to the inert matrix. Also, the current detected while using the spreading resistance mode (Figure 5) correspond to the ionically conductive regions on the surface of the membrane. The current will be detected only in the regions where there is a continuous interconnected ionic pathway from the ionic groups on the surface of the membrane to the ionomer existing at the catalyst/membrane interface. Nafion 212 has more ionic clusters than the electrospun membrane as evident from the intense purple (in color) or dark shaded region in the phase contrast image (Figure 4b) and higher electrical current in the surface spreading resistance image (Figure 5). A smaller scale for electrical current was used in the surface spreading resistance image of electrospun membrane to allow one to observe the PFSA fibrous region and the inert polymer region. Fewer ionic clusters are to be expected because only a fraction of the electrospun composite membrane's surface (Figure 5) consists of Nafion. Since only a fraction of the electrospun membrane surface is composed of the PFSA phase, and if we can assume that interior part of the membrane has the same

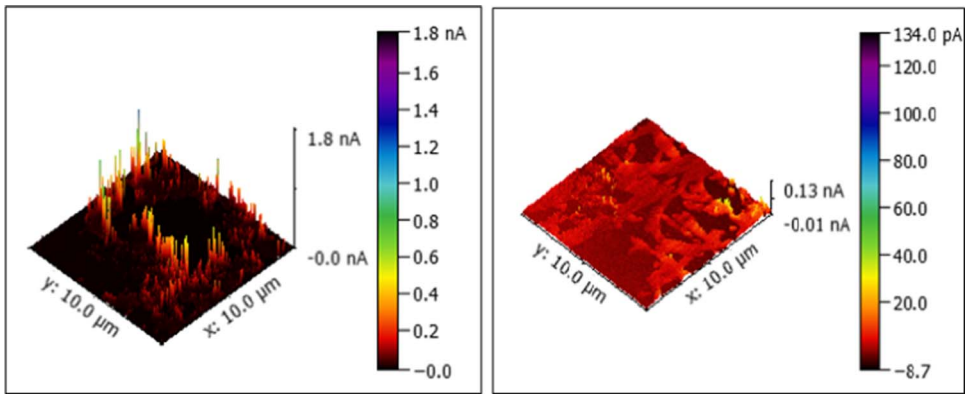

Figure 5. AFM images showing surface spreading resistance of Nafion (left) and dual fiber electrospun composite membrane (right) with color scales representing the currents measured.

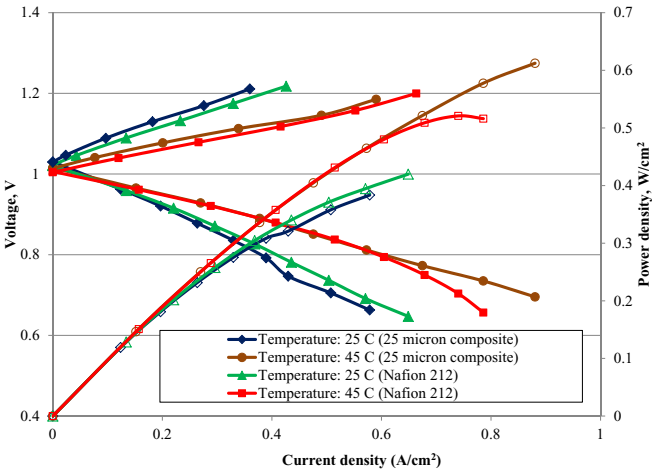

Figure 6. Performance (voltage: solid markers and power density: open markers) comparison between Nafion 212 and 25 micron thick dual fiber electrospun composite membranes at 25°C and 45°C.

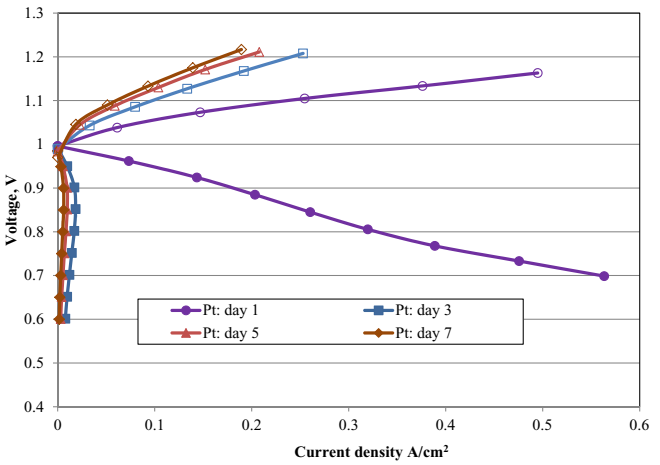

Figure 8. A week-long stability study with Pt as a H_2 electrocatalyst in a H_2-Br_2 fuel cell (cell performance measured on days 1, 3, 5, and 7) at room temperature (~22°C).

distribution, the crossover rate of Br_2 and Br^- per total area of the membrane will be considerably reduced. The crossover rate of Br_2 and Br^- of these electrospun composite membranes was also lower than that of the conventional Nafion membranes because the PFSA phase does not swell as much since it is restricted by the inert PPSU phase.[34]

The thickness of the electrospun membranes was optimized to approximately match the area specific resistance of the Nafion membranes. The preliminary performance of these electrospun membranes compared with that of the commercial Nafion membranes are shown in Figures 6 and 7. As shown in Figures 6 and 7, the performance of both 25 μm and 65 μm thick electrospun membranes are either comparable or slightly better compared to that of Nafion 212 and Nafion 115 membranes at 25°C and 45°C. At 45°C, the maximum power densities of 25 μm and 65 μm electrospun membranes were 0.61 A/cm^2 and 0.45 A/cm^2 compared to 0.52 A/cm^2 and 0.41 A/cm^2 obtained with Nafion 212 and Nafion 115 membranes. The sharp drop in the discharge performance for the fuel cell stack with Nafion 212 membrane at 45°C may be attributed to the dehydration of the ionomer in the hydrogen catalyst layer and the hydrogen side of the MEA due to inadequate anode gas humidification. Note that, water is dragged from the hydrogen side to the bromine side during discharge, and since Nafion 212 is thicker (~50 μm) than the composite membrane (~25 μm), it is more likely to become dehydrated at higher current densities than the composite membrane. The preliminary fuel cell performances obtained with electrospun membranes were on par with the commercially available Nafion membranes and hence look very promising for future studies. Also, the lower permeability of unwanted species associated with the electrospun membranes as described in previous studies is an additional benefit.[34,35]

Stability studies.— In this section, the stability of Pt and Rh_xS_y electrocatalysts in a H_2-Br_2 fuel cell was examined. Figures 8 and 9 show the performance curves obtained with Pt/C and Rh_xS_y/C catalysts over a week. As explained in the Experimental section, the H_2 flow was shut off and HBr/Br_2 electrolyte was stored in the Br_2 electrode between the subsequent fuel cell experiments. As shown in Figure 8, the discharge performance of the fuel cell was significantly reduced beyond day 1 due to the exposure of Pt catalyst layer in the H_2 electrode to Br_2, HBr^-, and HBr_3^- species. The Pt catalyst layer was both poisoned and corroded by the bromine and bromide species that crossed over from the Br_2 electrode to the H_2 electrode. The poisoning occurs due to the adsorption of Br^- species onto the active Pt catalyst sites.[21,39] As a result, the hydrogen atoms were deprived of active catalyst sites for reaction. Also, the Pt catalyst was corroded in the presence of Br_2 and Br_3^- species leading to the loss of active sites

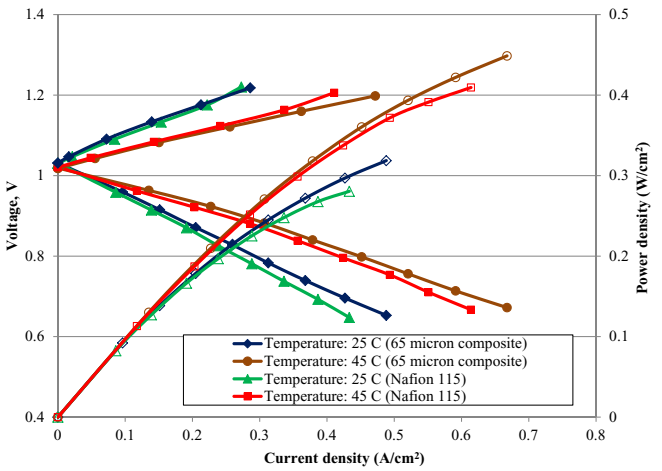

Figure 7. Performance (voltage: solid markers and power density: open markers) comparison between Nafion 115 and 65 micron thick dual fiber electrospun composite membranes at 25°C and 45°C.

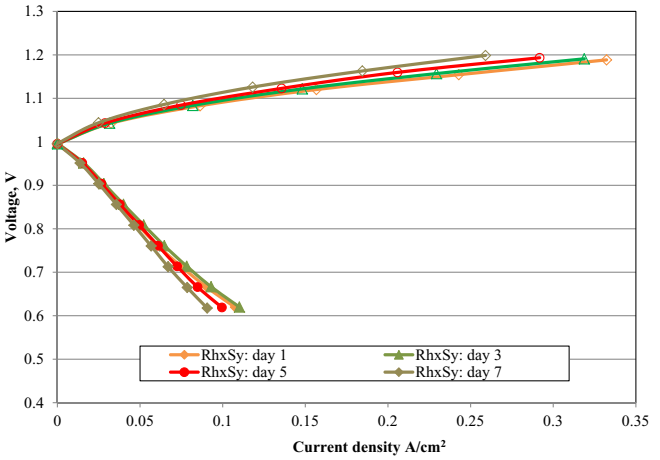

Figure 9. A week-long stability study with Rh_xS_y as a H_2 electrocatalyst in a H_2-Br_2 fuel cell (cell performance measured on days 1, 3, 5, and 7) at room temperature (~22°C).

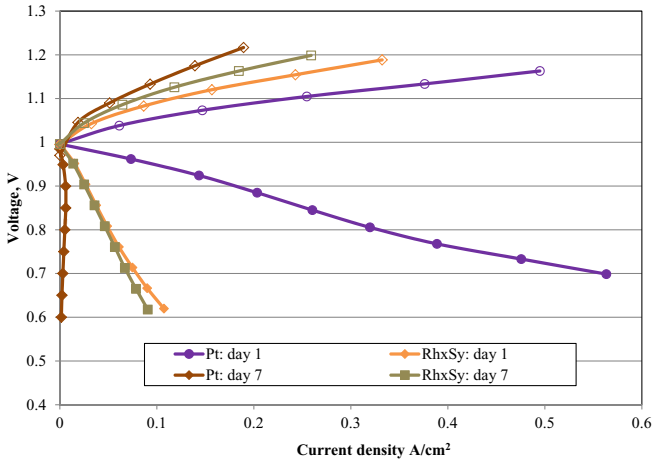

Figure 10. Comparing the stability of Pt and Rh_xS_y electrocatalysts on days 1 and 7 in a H_2-Br_2 fuel cell at room temperature (~22°C).

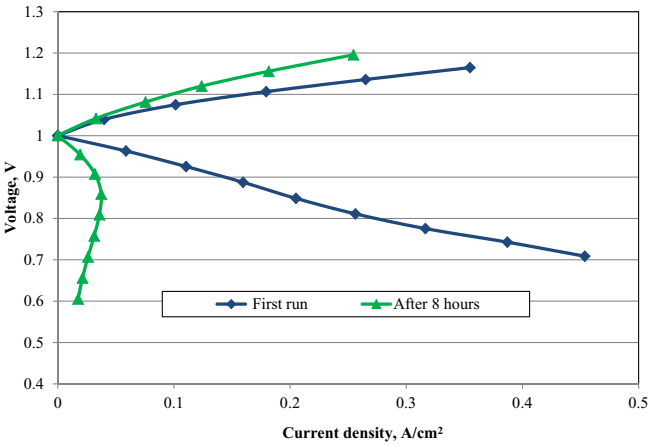

Figure 11. Stability study of Pt as a H_2 electrocatalyst in a H_2-Br_2 fuel cell with H_2 pump shut off (H_2 side was not pressurized between the two runs) at room temperature (~22°C).

for the electrochemical reactions to occur. The discharge performance obtained on day 3 and beyond was severely affected due to the combined effect of poisoning and corrosion. However, the effect of HBr and Br_2 crossover was not too severe in the charge direction compared to that in the discharge direction as seen in Figure 8. This is due to the fact that the poisoning effect is reversible since the adsorbed Br^- species can be removed at hydrogen evolution potentials and eventually flushed out by the H_2 gas flowing through the electrode.[39] The charge performances beyond day 1 show significantly higher overpotential which may be attributed to the permanent loss of platinum due to the dissolution of Pt catalyst. A continual decrease in charge performance on day 3 and beyond was observed as the platinum catalyst in the hydrogen electrode was further exposed to the HBr/Br_2 solution.

The performance of the fuel cell stack with Rh_xS_y shown in Figure 9 was almost unaffected by the crossover of Br_2, Br^-, and Br_3^- species. The slight decrease in both discharge and charge performance beyond day 1 could be attributed to dissolution of any free Rh metal present in the Rh_xS_y catalyst upon interacting with the crossover species.[22] Figure 10 compares the performance of Pt and Rh_xS_y catalysts on days 1 and 7. As shown in Figure 10, the charge performance of Rh_xS_y on day 1 was comparable to that of Pt whereas the discharge performance of Rh_xS_y was quite low. However, the discharge performance of the fuel cell with Rh_xS_y catalyst was unaffected over the week-long period of testing, which shows the superior stability of the Rh_xS_y catalyst over Pt. Currently, efforts are being undertaken towards understanding the hydrogen oxidation electrochemistry as well as improving the hydrogen oxidation activity of the Rh_xS_y catalyst material.

The following sections discuss the feasibility of the Pt catalyst in a H_2-Br_2 fuel cell fixture. In the first case study, two fuel cell stacks were assembled and tested under different experimental conditions. Figure 11 shows the two performance curves acquired with the first fuel cell stack, where the H_2 was shut off (H_2 side was not pressurized) in between the runs. The time period between the two runs was 8 hours. The fuel cell was allowed to stay at rest condition for the entire 8 hours between the two runs. As expected, the fuel cell performance was affected due to Br_2 and Br^- crossover. Since there was no recirculation of pressurized H_2 on the other side, the Br_2 and Br^- species were able to crossover with little resistance. A huge drop in discharge performance was observed after 8 hours. Based on the work done by Xu et al., bromide adsorption is voltage dependent and is believed to increase as the voltage at the H_2 electrode becomes more positive leading to higher adsorption of bromide and higher equilibrium potential.[39] This positive shift in the hydrogen equilibrium potential causes the current density to decrease resulting in poor performance.[11] Note that Br_2 in the presence of H_2 is converted immediately to Br^-. So, most of the adsorbed species will be Br^-, not Br_2, when H_2 is present. Overall, the catalyst is both poisoned and corroded in the absence of H_2 recirculation.

Figure 12 shows the results obtained with the second stack, where the pressurized H_2 gas was continuously circulated between the two performance runs. As shown in Figure 12, the performance was unaffected due to the resistance offered by the continuous H_2 recirculation against the crossover of Br_2 and Br^- species. It is suspected that when H_2 pressure is maintained while the HBr/Br_2 pump is stopped, the H_2 gas will push the HBr/Br_2 solution away from the membrane/bromine electrode interface thus reducing the chance for HBr/Br_2 electrolyte to crossover to the H_2 side. Furthermore, there is a concern that even with hydrogen pressure in the hydrogen compartment, the diffusion rate of hydrogen through the electrolyte, created in the hydrogen electrode by cross-over of bromine solution, to the platinum surface may not be fast enough to keep the platinum surface protected from bromine and bromide ions, especially during open circuit. The study by Cho et al. shows reduced platinum dissolution rate when a hydrogen atmosphere or hydrogen evolution potential was applied to the hydrogen electrode during rest or standby.[12] In conclusion, the continuous H_2 recirculation offers resistance towards the species crossover, which in turn prolongs the life of the fuel cell. However, the continuous gas recirculation in not practical and hence not a suitable permanent solution to avoid crossover issues.

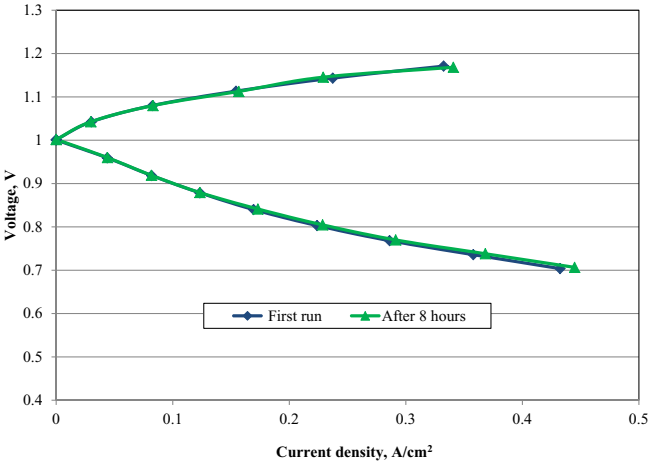

Figure 12. Stability study of Pt as a H_2 electrocatalyst in a H_2-Br_2 fuel cell with H_2 pump on (H_2 pressure maintained between the two runs) at room temperature (~22°C).

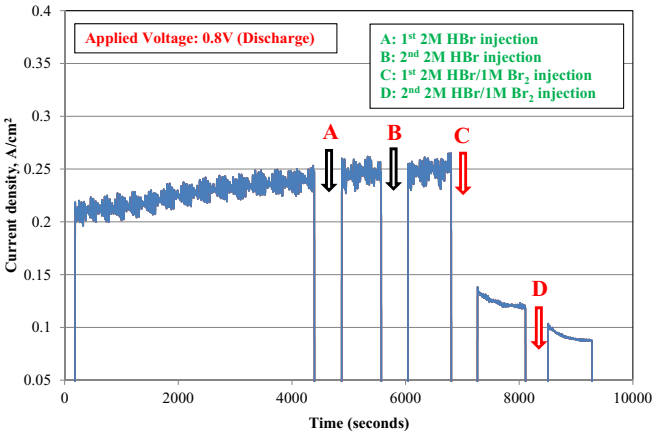

Figure 13. Effect of HBr (locations A and B) and HBr/Br_2 (locations C and D) injections on the discharge performance of a H_2-Br_2 fuel cell held at a constant voltage, 0.8V at room temperature (~22°C).

The next case study involves injecting HBr and HBr/Br_2 solutions directly into the H_2 electrode to simulate the Br^- and Br_2 species crossover. The objective of this study, which is designed to bypass the long wait time associated with the slow crossover rate of the aqueous species from the bromine side to the hydrogen side, was to observe the immediate effect of Br_2 and Br^- species crossover on the fuel cell discharge performance. The testing protocol is explained in detail in the Experimental section. Figure 13 shows the results obtained in this study. Initially, HBr alone was injected to observe the impact of Br^- ion crossover. A 2M HBr solution was injected twice and for each injection, the fuel cell was allowed to stay at OCV (for approximately 8 minutes) for the Br^- ions to interact with the Pt catalyst layer. As shown in Figure 13, the performance was unaffected after the two injections (A & B). Since the microporous layer of the H_2 electrode is extremely hydrophobic, it is highly improbable for the Br^- ions to reach the Pt catalyst layer. Hence, the performance of the fuel cell was not affected. However, the performance of the fuel cell was affected once a mixture of HBr and Br_2 is injected (see Figure 13 points C & D). The performance deteriorated with each injection. Even though liquid could not penetrate into the highly hydrophobic microporous layer, the Br_2 species in vapor state could still diffuse through the microporous layer to contact the Pt catalyst layer and, subsequently, poison and corrode the platinum catalyst. This case study suggests two major conclusions. First, there is an instantaneous effect once the Br_2 species interacts with the Pt catalyst. Second, the effect of Br_2 vapor on the Pt catalyst is as severe as liquid bromine or bromide ions. The occurrence of events such as emergency shutdowns or having to idle the system prior to complete degradation of the H_2-Br_2 fuel cell still needs to be studied.

Conclusions

The attractive features as well as some of the material related issues corresponding to the H_2-Br_2 fuel cell are discussed in this study. Preliminary fuel cell test results clearly highlighted the immense energy storage potential of the H_2-Br_2 fuel cell, which is a result of the highly reversible electrochemical reactions associated with the reactants used in this system. The novel dual fiber electrospun composite membranes (PFSA/PPSU) have been tested in an actual H_2-Br_2 fuel cell. The preliminary performance of these electrospun membranes look quite promising indicating that they might be an alternative to Nafion membranes. The Pt catalyst is prone to corrosion and poisoning due to the crossover of Br_2 and Br^- species from the Br_2 electrode to the H_2 electrode. Both Pt and Rh_xS_y catalysts were evaluated in an actual fuel cell to determine their activity and stability. The stability of Rh_xS_y in HBr/Br_2 environment was excellent compared to that of Pt. However, the H_2 oxidation activity of Rh_xS_y was quite low and needs to be improved for it to be used as an electrocatalyst in the H_2 electrode. The feasibility of using a Pt catalyst under different experimental conditions was evaluated. The lifetime of the fuel cell could be prolonged through continuous flow of H_2 gas and keeping the H_2 electrode pressurized. Using an alternative H_2 electrocatalyst that is stable and active is still the best option to solve the crossover issues since there is a possibility of a Pt catalyst system design failing under certain situations such as loss of hydrogen environment.

Acknowledgments

The authors acknowledge the financial support of this work by the National Science Foundation through grant no. EFRI-1038234.

References

1. Adam Z. Weber, Matthew M. Mench, Jeremy P. Meyers, Philip N. Ross, Jeffrey T. Gostick, and Qinghua Liu, *J. Appl. Electrochem.*, **41**, 1137 (2011).
2. C. Ponce de Leon, A. Frias-Ferrer, J. Gonzalez-Garcia, D. A. Szanto, and F. C. Walsh, *J. Power Sources*, **160**, 716 (2006).
3. M. Skyllas-Kazacos, M. H. Chakrabarti, S. A. Hajimolana, F. S. Mjalli, and M. Saleem, *J. Electrochem. Soc.*, **158**(8), R55 (2011).
4. T. Nguyen and R. Savinell, *Electrochemical Society Interface*, **19**(3), 54 (2010).
5. Werner Glass and G. H. Boyle, *Advances in chemistry series*, **47**, 203 (1965).
6. R. S. Yeo and D. T. Chin, *J. Electrochem. Soc.*, **127**(3), 549 (1980).
7. G. G. Barna, S. N. Frank, T. H. Teherani, and L. D. Weedon, *J. Electrochem. Soc.*, **131**(9), 1973 (1984).
8. V. Livshits, A. Ulus, and E. Peled, *Electrochemistry Communications*, **8**, 1358 (2006).
9. Kyu Taek Cho, Paul Ridgeway, Adam Z. Weber, Sophia Haussener, Vincent Battagalia, and Venkat Srinivasan, *J. Electrochem. Soc.*, **159**(11), A1806 (2012).
10. Haley Kreutzer, Venkata Yarlagadda, and Trung Van Nguyen, *J. Electrochem Soc.*, **159**(7), F331 (2012).
11. Haley M. Kreutzer, MS Thesis, University of Kansas, Lawrence, KS, USA, May 2012.
12. Michael C. Tucker, Kyu Taek Cho, Adam Z. Weber, Guangyu Lin, and Trung Van Nguyen, *J. Appl. Electrochem.*, **45**, 11 (2015).
13. William A. Braff, Martin Z. Bazant, and Cullen R. Buie, *Nature Communications*, **4**, 2346 (2013).
14. Marc-Antoni Goulet and Erik Kjeang, *J. Power Sources*, **260**, 186 (2014).
15. E. R. Choban, J. S. Spendelow, L. Gancs, A. Wieckowski, and P. J. A. Kenis, *Electrochimica Acta*, **50**, 5390 (2005).
16. S. W. Choi, Y. Z. Fu, Y. R. Ahn, S. M. Jo, and A. Manthiram, *J. Power Sources*, **180**, 167 (2008).
17. Ryouhei Takemori and Hiroyoshi Kawakami, *J. Power Sources*, **195**, 5957 (2010).
18. Takuya Tamura and Hiroyoshi Kawakami, *Nano Lett.*, **10**, 1324 (2010).
19. E. Aleksandrova, S. Hink, R. Hiesgen, and E. Roduner, *J. Physics: Condensed Matter*, **23**, 234109 (2011).
20. P. J. James, J. A. Elliott, T. J. McMaster, J. M. Newton, A. M. S. Elliott, S. Hanna, and M. J. Miles, *J. of Materials Science*, **35**, 5111 (2000).
21. M. Goor-Dar, N. Travitsky, and E. Peled, *J. Power Sources*, **197**, 111 (2012).
22. N. Singh, S. Mubeen, J. Lee, H. Metiu, M. Moskovits, and E. W. McFarland, *Energy Environ. Sci.*, **7**, 978 (2014).
23. Joseph M. Ziegelbauer, Andrea F. Gulla, Cormac O. Laoire, Christian Urgeghe, Robert J. Allen, and Sanjeev Mukerjee, *Electrochimica Acta*, **52**, 6282 (2007).
24. Dimitrios C. Papageorgopoulos, Fang Liu, and Olaf Conrad, *Electrochimica Acta*, **52**, 4982 (2007).
25. Andrea F. Gulla, Lajos Gancs, Robert J. Allen, and Sanjeev Mukerjee, *Applied Catalysis A: General*, **326**, 227 (2007).
26. Chen Jin, Wei Xia, Tharamani Chikka Nagaiah, Junsong Guo, Xingxing Chen, Michael Bron, Wolfgang Schuhmann, and Martin Muhler, *Electrochimica Acta*, **54**, 7186 (2009).
27. Joseph M. Ziegelbauer, Daniel Gatewood, Andrea F. Gulla, Maxime J.-F. Guinel, Frank Ernst, David E. Ramaker, and Sanjeev Mukerjee, *J. Phys. Chem.*, **113**, 6955 (2009).
28. Jacob Bonde, Poul G. Moses, Thomas F. Jaramillo, Jens K. Norskov, and Ib Chorkendorff, *Faraday Discussions*, **140**, 219 (2008).
29. Anna Ivanovskaya, Nirala Singh, Ru-Fen Liu, Haley Kreutzer, Jonas Baltrusaitis, Trung Van Nguyen, Horia Metiu, and Eric McFarland, *Langmuir*, **29**, 480 (2013).
30. Trung Van Nguyen, Haley Kreutzer, Venkata Yarlagadda, Eric McFarland, and Nirala Singh, *ECS Transactions*, **53**(7), 75 (2013).
31. Kyu Taek Cho, Paul Albertus, Vincent Battaglia, Aleksander Kojic, Venkat Srinivasan, and Adam Z. Weber, *Energy Technol.*, **1**, 596 (2013).
32. Venkata Yarlagadda and Trung Van Nguyen, *J. Electrochem Soc.*, **160**(6), F535 (2013).
33. David Wood III, Jung S. Yi, and Trung V. Nguyen, *Electrochimica Acta*, **43**, 3795 (1998).
34. J. W. Park, R. Wycisk, and P. N. Pintauro, *ECS Transactions*, **50**(2), 1217 (2012).
35. J. B. Ballengee and P. N. Pintauro, *Macromolecules*, **44**, 7307 (2011).
36. T. V. Nguyen, M. V. Nguyen, G. Lin, N. Rao, X. Xie, and D. Zhu, *Electrochemical and Solid State Letters*, **9**, A88 (2006).
37. X. Xie, O. Kwon, D.-M. Zhu, T. Van Nguyen, and G. Lin, *J. Physical Chemistry B*, **111**(22), 6134 (2007).
38. Venkata Yarlagadda and Trung Van Nguyen, *ECS Transactions*, **58**(36), 25 (2014).
39. Jing Xu and Daniel Scherson, *Anal. Chem.*, **85**, 2795 (2013).